Materials and Methods

Cell isolation: All protocols involving animals conform with the *Guide for the Care and Use of Laboratory Animals* published by the US National Institutes of Health (NIH Publication No. 85–23, revised 1996) and were approved by the Johns Hopkins Animal Care and Use Committee. Guinea pig ventricular myocytes were isolated by enzymatic digestion as described previously.[1]

Whole-Cell Patch-Clamp: Myocytes were loaded in a heated chamber (37°C) on the stage of a fluorescence microscope (Nikon Eclipse TE300) and superfused with Tyrode´s solution containing (in mmol/L): NaCl 130, KCl 5, $MgCl_2$ 1, Na-HEPES 10, $CaCl_2$ 2, glucose 10, pyruvate 2, ascorbic acid 0.3; pH 7.4. Myocytes were whole-cell patch-clamped with 2-4 MΩ pipettes and equilibrated with a pipette solution containing (in mmol/L) K-glutamate 130, KCl 19, $MgCl_2$ 0.5, Na-HEPES 5, HEPES 10, Mg-ATP 5, and indo-1 (penta-K^+ salt; Molecular Probes) 0.075 for about 10 minutes. As indicated 1 μM CGP-37157 (mNCE inhibitor), 2 mM K_2HPO_4, or 100 nM Ru360 (MCU inhibitor) were added into the pipette solutions, except in the case of the field-stimulation experiments (cells not subjected to patch clamp) shown in Figure 5, where 10uM CGP-37157 was added to the bath solution. Membrane currents were recorded as described previously,[2] in whole-cell voltage clamp mode (Axopatch 200A amplifier, Digidata 1200B interface, Axon Instruments). Electrophysiological signals were acquired, stored and analyzed using custom-written software.

Fluorescence recording: To monitor $[Ca^{2+}]_m$, cells were incubated with rhod-2 acetoxymethyl esther (rhod-2 AM, 3 μmol/L; Molecular Probes; dissolved in DMSO +10% pluronic acid) in DMEM for 1 h at 37°C, and followed by 1 h deesterification in rhod-2-free DMEM. Rhod-2 was excited at λ_{exc}= 540 nm for 200 ms at 4 Hz, and emission was recorded at λ_{em}= 605 nm with photomultipliers. The cytosolic component of the dye was removed by patch clamp with a rhod-2 free pipette solution, as described previously.[2]

The endogenous autofluorescence of mitochondrial NADH was excited at λ_{exc}= 360 nm and its emission recorded at λ_{em}=450-485 nm in the same cells, Excitation filters for rhod-2 and NADH were switched every 10 pulses.

$[Na^+]_i$ was measured ratiometrically using SBFI in resting cells that were not patch-clamped. Cells were incubated with 10 μmol/L SBFI-AM (Molecular Probe) in Tyrodes' solution for 1 h at room temperature followed by 1 h deesterification in SBFI-free Tyrodes' solution. SBFI was excited alternatively at 340 nm and

380 nm, and emission was recorded at 530 nm with photomultiplier. SBFI fluorescence was calibrated as described by others.[3, 4] Briefly, after application of 7.5 μmol/L gramicidin D, an ionphore, and 100 μmol/L strophanthidin, an inhibitor of Na^+-K^+ pump, cells were superfused with solutions containing various Na^+ concentrations. The observed values of the 340 nm/380 nm excitation ratio were used to solve for the parameters, R_{min}, R_{max}, and $K_d \times \beta$, in the standard equation:

$$[Na^+]_i = K_d \times \beta \times (R-R_{min})/(R_{max}-R)$$

where R is the observed 340/380 nm excitation ratio, R_{min} is the ratio at 0 mmol/l $[Na^+]_i$, R_{max} is the ratio at saturating $[Na^+]_i$, K_d is the dissociation constant, and β is the ratio of the excitation efficiencies of free SBFI to Na^+-bound SBFI at 380 nm.

Cells were recorded in the presence of 100 nM isoproterenol using the following protocol: 100s recording at rest followed by 100s recording during 4 Hz stimulation, and then return to the resting state.

Rhod-2 fluorescence was normalized to the F0, which was recorded before rupturing the cell membrane during the establishment of the whole cell recording. NADH level was expressed as percent reduction of the NADH/NAD^+ pool, which was calibrated by adding the mitochondrial uncoupler 5 μM FCCP (0 %) and the cytochrome oxidase inhibitor 4 mM NaCN (100%) at the end of each recording.

Heart failure and functional evaluation: Adult male Hartley guinea-pigs (250-300 g) were anesthetized and intubated. Ascending aortic constriction was produced by tying a suture around the ascending aorta using an 18-gauge needle as a spacer, which was then removed. When animals were breathing spontaneously after the procedure, buprenex (0.05mg/kg) was administered for analgesia and animals were observed until full recovery. Animals underwent echocardiography every 2 weeks after surgery. Left ventricular ejection fraction (EF) was calculated with VisualSonics V1.3.8 software from 2D long-axis views. When a decrease in EF was observed (after ~6-8 weeks), animals were euthanized, heart weight/tibia length was measured, and cardiomyocytes were isolated.

Statistical Analysis: Values are given as means ±SEM. Statistical analysis was performed using Student´s t-test for unpaired samples. Fitting of the decay of mitochondrial Ca^{2+} and smoothing of $[Ca^{2+}]$-transients were performed with Origin software (Originlab, Northampton, MA). $P<0.05$ was considered significant.

Results

Effect of $[Na^+]_i$, CGP-37157, and Pi on $[Ca^{2+}]_m$ decay: $[Ca^{2+}]_m$ transients at the beginning of stimulation with different treatments were analyzed. The time to 50% decay (D50) of $[Ca^{2+}]_m$ was measure as indicated in Figure S1, and the result is displayed in Table S.

Effect of cyclosporine A on $[Ca^{2+}]_m$ efflux: Although our analysis of $[Ca^{2+}]_m$ transients demonstrated the effects of elevated $[Na^+]_i$ and CGP-37157 on $[Ca^{2+}]_m$ efflux, the slow decay of diastolic $[Ca^{2+}]_m$ during recovery after stimulation was, remarkably, not affected by $[Na^+]_i$ or CGP-37157. To test whether the mitochondrial permeability transition pore (mPTP) might play a role in this $[Ca^{2+}]_m$ decay, we applied 0.2 μM cyclosporine A (CsA) to inhibit mPTP. In cells with 5 mM $[Na^+]_i$ and CGP-37157, CsA further increased $[Ca^{2+}]_m$ accumulation (F/F0 of rhod-2 is 1.80±0.20 at the end of stimulation and 1.41±0.10 after recovery) (Fig. S2A). However, the time constant of $[Ca^{2+}]_m$ decay during recovery after stimulation was not significantly altered (Fig. S2B). The results suggest that mPTP activation during stimulation may partially limit $[Ca^{2+}]_m$ accumulation, but that mPTP is not directly involved in the mechanism of Ca^{2+} removal from the matrix after Ca^{2+} loading by rapid stimulation.

Effect of glutamate and pyruvate on NADH production: In our experiments, 130 mM K-glutamate was contained in pipette solution and 2 mM pyruvate was provided in perfusate solution because, based on the work in our lab and others, K-glutamate can provide a better ionic and osmotic environment for cardiac myocyte and pyruvate is helpful to maintain mitochondrial membrane potential. However, glutamate and pyruvate may also have some effects on NADH production. Glutamate is a substrate of TCA cycle and pyruvate can regulate pyruvate dehydrogenase (PDH) through PDH kinase. To evaluate the effects of glutamate and pyruvate on NADH production, we replaced K-glutamate with KCl in pipette solution and omitted pyruvate in perfusate solution, and recorded NADH fluorescence using same protocol in cells with 5 (Fig. S3A) and 15 (Fig. S3B) mM Na^+. In cells with 5 mM Na^+, NADH level was maintained during stimulation (pre-stimulation: 78.3%±1.1; end-stimulation: 76.0%±2.1); In cells with 15 mM Na^+, NADH level during stimulation decreased at a similar level to that of recording with glutamate and pyruvate (the difference between pre-stimulation and end-stimulation is 22.5%±3.3 in KCl and pyruvate free condition and 19.3%±5.3 in K-glutamate and pyruvate condition, p=0.3).

Discussion

Mitochondrial Ca^{2+} efflux

Surprisingly, the decay rate of accumulated $[Ca^{2+}]_m$ during the recovery after stimulation did not show an obvious dependence on Na^+ or CGP-37157. Experiments with 5 or 15 mM $[Na^+]_i$, with or without CGP-37157, had no significant difference in the rate of $[Ca^{2+}]_m$ decay after stimulation, though low $[Na^+]_i$ or CGP-37157 were associated with a higher $[Ca^{2+}]_m$ level after recovery. This observation suggests that other mitochondrial Ca^{2+} efflux pathways may be involved. Ca^{2+}/nH^+ exchanger is a Na^+-independent $[Ca^{2+}]_m$ efflux mechanism identified by Gunter et al.[5] However this mechanism is unlikely to play a significant role in our study due to its low activity in cardiac tissue.[6] Ca^{2+} and various other factors induce the opening of mPTP, which allows the transit of small molecules (<1.5 kD). Ichas and coworkers demonstrated that transitory opening of mPTP as a possible mechanism for $[Ca^{2+}]_m$ efflux.[7] To investigate the role of mPTP, we applied 0.2-0.5 μM CsA to inhibit mPTP. Our results showed a slight increase of $[Ca^{2+}]_m$ accumulation with no significant change in the rate of $[Ca^{2+}]_m$ decay after stimulation (Fig. 2H), suggesting that mPTP may open during rapid stimulation to limit $[Ca^{2+}]_m$ accumulation, probably as a result of some mitochondria experiencing PTP-mediated depolarization of $\Delta\Psi_m$ to decrease the driving force for Ca^{2+} entry. mPTP did not, however, contribute to the slow $[Ca^{2+}]_m$ decay upon cessation of stimulation. Another possible mechanism could be Ca^{2+} efflux through reversal of uptake pathways including MCU and mRyR. This is unlikely, since Ca^{2+} movements are driven by the electrochemical gradient, which still strongly favors Ca^{2+} influx under the conditions of our experiments.[4] Reversal of MCU has been proposed to contribute to $[Ca^{2+}]_m$ efflux when $\Delta\Psi_m$ is dissipated, but coupled mitochondria can maintain millimolar levels of Ca^{2+} in matrix. Furthermore, although $[Ca^{2+}]_m$ accumulation was less in the presence of Ru360, some Ca^{2+} was taken up, and its decay upon ceasing the stimulation was not obviously altered. This finding also argues against a role for MCU or mRyR in the slow efflux phase. To more specifically investigate whether mRyR was involved in $[Ca^{2+}]_m$ efflux, we inhibited mRyR inhibition with 1mM tetracaine, and these experiments did not show any effect of mRyR inhibition on the rate of $[Ca^{2+}]_m$ decay (data not shown). The mechanism will require further investigation to resolve in the future.

Supplemental References

1. O'Rourke B, Ramza BM, Marban E. Oscillations of membrane current and excitability driven by metabolic oscillations in heart cells. *Science (New York, N.Y.* Aug 12 1994;265(5174):962-966.

2. Maack C, Cortassa S, Aon MA, Ganesan AN, Liu T, O'Rourke B. Elevated cytosolic Na+ decreases mitochondrial Ca2+ uptake during excitation-contraction coupling and impairs energetic adaptation in cardiac myocytes. *Circulation research.* Jul 21 2006;99(2):172-182.

3. Donoso P, Mill JG, O'Neill SC, Eisner DA. Fluorescence measurements of cytoplasmic and mitochondrial sodium concentration in rat ventricular myocytes. *The Journal of physiology.* Mar 1992;448:493-509.

4. Harootunian AT, Kao JP, Eckert BK, Tsien RY. Fluorescence ratio imaging of cytosolic free Na+ in individual fibroblasts and lymphocytes. *The Journal of biological chemistry.* Nov 15 1989;264(32):19458-19467.

5. Gunter TE, Chace JH, Puskin JS, Gunter KK. Mechanism of sodium independent calcium efflux from rat liver mitochondria. *Biochemistry.* Dec 20 1983;22(26):6341-6351.

6. Gunter TE, Buntinas L, Sparagna G, Eliseev R, Gunter K. Mitochondrial calcium transport: mechanisms and functions. *Cell calcium.* Nov-Dec 2000;28(5-6):285-296.

7. Ichas F, Jouaville LS, Mazat JP. Mitochondria are excitable organelles capable of generating and conveying electrical and calcium signals. *Cell.* Jun 27 1997;89(7):1145-1153.

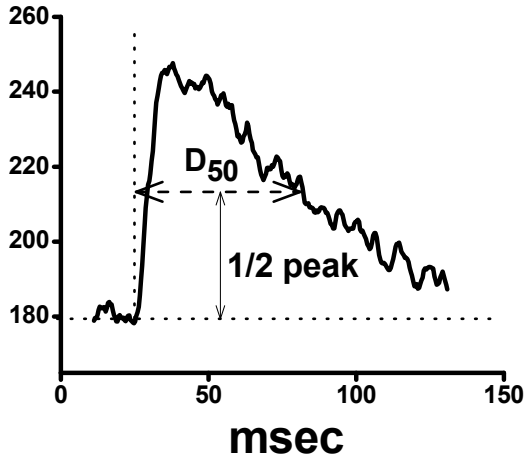

Measurement of D50 for $[Ca^{2+}]_m$ decay

		Mean	SEM
5 Na	Control	46.2	3.7
	CGP	62.1*	5.3
	Pi	72.8*	9.8
15Na	Control	38.5	3.9
	CGP	54.3*	5.8
	Pi	57.2*	5.8

* $p<0.05$ while compared to control

Figure S1 /Table S1. Effect of $[Na^+]_i$, CGP-37157, and Pi on $[Ca^{2+}]_m$ decay $[Ca^{2+}]_m$ transients at the beginning of stimulation with different treatments were analyzed. The time to 50% decay (D50) of $[Ca^{2+}]_m$ was measure as indicated in Figure S1, and the result is displayed in Table S1.

Figure S2

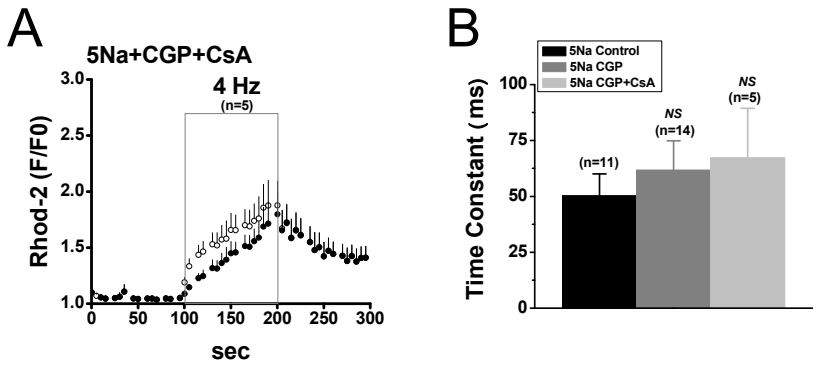

Figure S2. Effect of cyclosporine A on $[Ca^{2+}]_m$ efflux

Although our analysis of $[Ca^{2+}]_m$ transients demonstrated the effects of elevated $[Na^+]_i$ and CGP-37157 on $[Ca^{2+}]_m$ efflux, the slow decay of diastolic $[Ca^{2+}]_m$ during recovery after stimulation was, remarkably, not affected by $[Na^+]_i$ or CGP-37157. To test whether the mitochondrial permeability transition pore (mPTP) might play a role in this $[Ca^{2+}]_m$ decay, we applied 0.2 μM cyclosporine A (CsA) to inhibit mPTP. In cells with 5 mM $[Na^+]_i$ and CGP-37157, CsA increased $[Ca^{2+}]_m$ accumulation (F/F0 of rhod-2 is 1.80±0.20 at the end of stimulation and 1.41±0.10 after recovery) (Fig. S2A). However, the time constant of $[Ca^{2+}]_m$ decay during recovery after stimulation was not significantly altered (Fig. S2B). The results suggest that mPTP activation during stimulation may partially limit $[Ca^{2+}]_m$ accumulation, but that mPTP is not directly involved in the mechanism of Ca^{2+} removal from the matrix after Ca^{2+} loading by rapid stimulation.

Figure S3

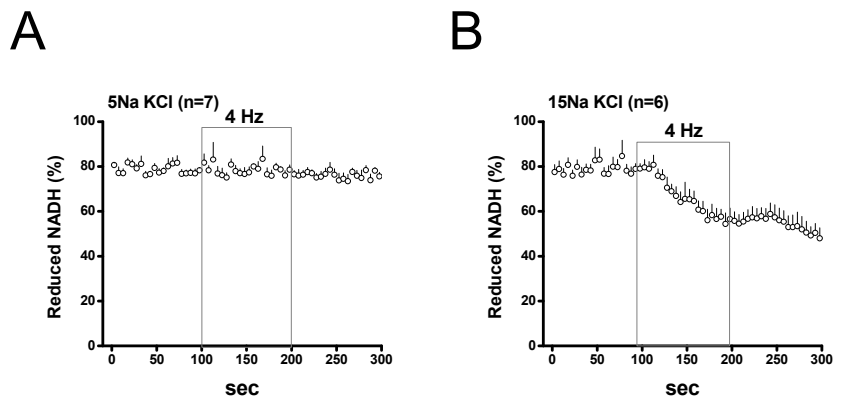

Figure S3. Effect of glutamate and pyruvate on NADH production
In the experiments shown in the paper, 130 mM K-glutamate was utilized in the pipette solution and 2 mM pyruvate was provided in perfusate . The glutamate is typically used in patch clamp experiments as a Cl^- substitute so that the normal Cl- equilibrium potential is maintained Erev(~ -55mV), while the pyruvate plus glucose is helpful to maintain mitochondrial membrane potential. However, glutamate and pyruvate may also have some effects on NADH production. Glutamate is a substrate of TCA cycle and pyruvate can regulate pyruvate dehydrogenase (PDH) through PDH kinase. To evaluate the effects of glutamate and pyruvate on NADH production, we replaced K-glutamate with KCl in pipette solution and omitted pyruvate in perfusate solution, and recorded NADH fluorescence using same protocol in cells with 5 (Fig. S3A) or 15 (Fig. S3B) mM Na^+. In cells with 5 mM Na^+, NADH level was maintained during stimulation (pre-stimulation: 78.3%±1.1; end-stimulation: 76.0%±2.1); In cells with 15 mM Na^+, NADH level during stimulation decreased to a similar level as that when recorded with glutamate and pyruvate (the difference between pre-stimulation and end-stimulation is 22.5%±3.3 in KCl and pyruvate free condition and 19.3%±5.3 in K-glutamate and pyruvate condition, p=0.3). Hence, the absence of these substrates did not affect the outcome of the experiments.

Figure S4

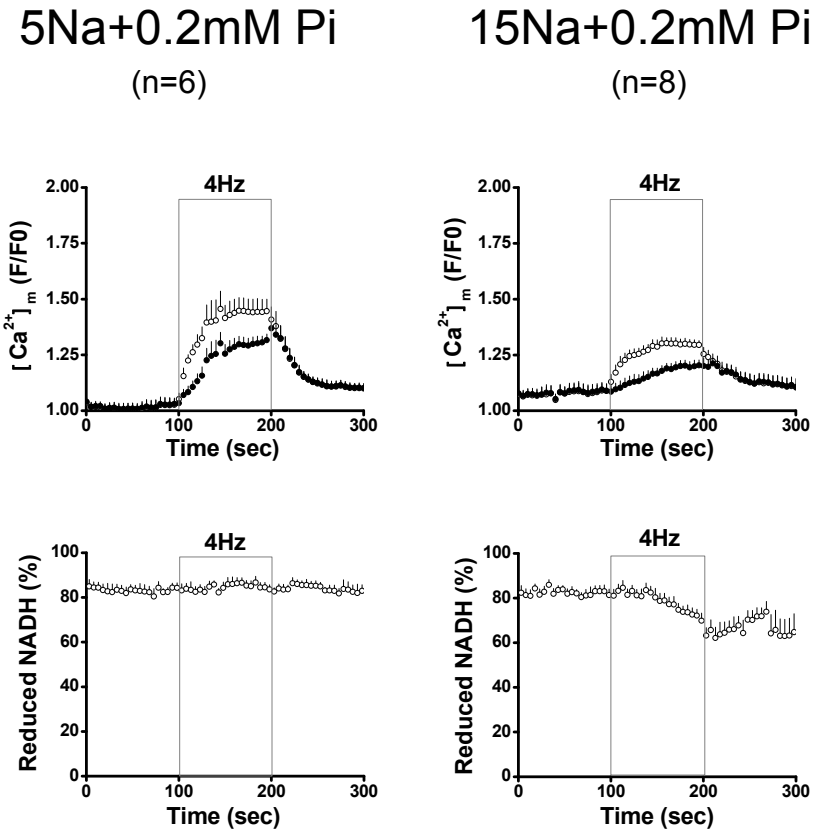

Figure S4. Effect $[Na^+]_i$ on $[Ca^{2+}]_m$ and NADH with 0.2 mmol/L P_i in pipette.
Inclusion of an intermediate level of P_i in the intracellular solution did not prevent the effect on NADH oxidation during pacing with 15 mM $[Na^+]_i$, although the response developed more slowly as compared to no added P_i. The results fell along the same correlation line as for other interventions that altered mitochondrial Ca^{2+} dynamics (see summary in Fig. 6 of paper).